INORGANIC CHEMISTRY FRONTIERS

RESEARCH ARTICLE

View Article Online
View Journal

Cite this: DOI: 10.1039/d6qi00325g

Selective C–O cleavage and C═O deoxygenation of carbamates and polyurethane catalyzed by organoactinide complexes

Tamer Saiaede,†[a] Ida Ritacco, †[b] Lucia Caporaso*[b,c] and Moris S. Eisen *[a]

The remarkable ability of actinide complexes to activate carbamates is presented in this study, exemplified by the carbamate hydroboration using various Th and U complexes. The activation mode involves the selective catalytic cleavage of the C–O bond and the deoxygenation of the double C═O bond, utilizing pinacolborane (HBpin) as a hydride source. The broad scope of the organoactinides allows us to perform the activation reaction with diverse structural and functional carbamates, offering a flexible strategy for the synthesis of complex amines and amino alcohols. For example, the synthesis of (–) ephedrine and other bioactive analog molecules was achieved in a one-pot, two-step reaction utilizing commercially available carbamate derivatives, including multigram-scale reactions. Additionally, the capability of actinide catalysts to facilitate late-stage modifications of drugs has been extensively studied, and various pharmaceutical compounds have been examined. Notably, we also present the homogeneous catalytic depolymerization of a polyurethane polymer, recycling it to its valuable diamine [Me–N(H)–R–N(H)–Me] through hydroboration followed by hydrolysis. The use of an organic-f-lanthanide compound is also presented as a comparison to the actinides to show their industrial applicability. To understand the reactivity of the actinide complexes, stoichiometric reactions, together with kinetic experiments, thermodynamic measurements, and deuterium labeling studies, were performed, allowing us to propose a mechanistic pathway. Computational DFT calculations further substantiate the proposed mechanism.

Received 18th February 2026,
Accepted 22nd April 2026

DOI: 10.1039/d6qi00325g

rsc.li/frontiers-inorganic

Introduction

Recently, considerable attention has been focused on the catalytic activity of organoactinide complexes.[1–3] Owing to their unique metal characteristics, such as 5f orbitals and large ionic size, these complexes can provide highly reactive metal centers capable of activating small molecules.[4–7] For example, the recent activation of small molecules such as N_2, H_2, CO, and CO_2 has been achieved using actinide complexes.[8–18] However, actinides are highly oxophilic centers, forming strong metal–oxygen bonds (U–O = 181.0 kcal mol^{-1} and Th–O = 208.0 kcal mol^{-1}). This makes their catalytic activities with oxygenated compounds particularly challenging.[19] In this context, the possibility of recycling a very reactive An–H (An = U, Th) moiety from a stable An–O motif was disclosed previously in our group using pinacolborane (HBpin) as the hydride source. The initial results of such recycling were presented in the catalytic hydroboration of ketones and aldehydes, indicating a proof of concept that organoactinide complexes can also catalyze such transformation.[20] The recycling capabilities of an An–H from their corresponding An–O moieties were extended toward more challenging carbonyl-containing compounds with lower polarizabilities.[21,22] Although aldehydes and ketones are easily hydroborated, for esters and amides it is more challenging, followed by carbamates and ureas, whose hydroboration is the most difficult due to their less polarized carbonyl groups.[22–27] In this regard, the thorium metallocene complex with highly electron-rich Cp* ligands ($Cp^*_2ThMe_2$) displayed the ability to induce the hydroboration of different amides with the concomitant deoxygenation to produce the corresponding amines (Fig. 1A, right side).[28] Interestingly, the coordinative unsaturated metallacycle thorium catalyst (**I**) is an active complex towards cleaving esters and carbonates (C═O reduction followed by a C–O bond cleavage), *via* their hydroboration (Fig. 1A, left side).[29,30] In addition, the use of thorium or uranium imidazolin-2-iminato complexes showed the ability to induce the deoxygenation of

[a]*Schulich Faculty of Chemistry, Technion – Israel Institute of Technology, Technion City, 3200008, Israel. E-mail: chmoris@technion.ac.il*
[b]*Dipartimento di Chimica e Biologia "Adolfo Zambelli", Università degli Studi di Salerno, Via Giovanni Paolo II, 132 – 84084 Fisciano, Salerno, Italy. E-mail: lcaporaso@unisa.it*
[c]*CNR-IOM, Consiglio Nazionale Delle Ricerche – Istituto Officina Dei Materiali, C/o SISSA, Trieste, 34136, Italy*
†These authors contributed equally.

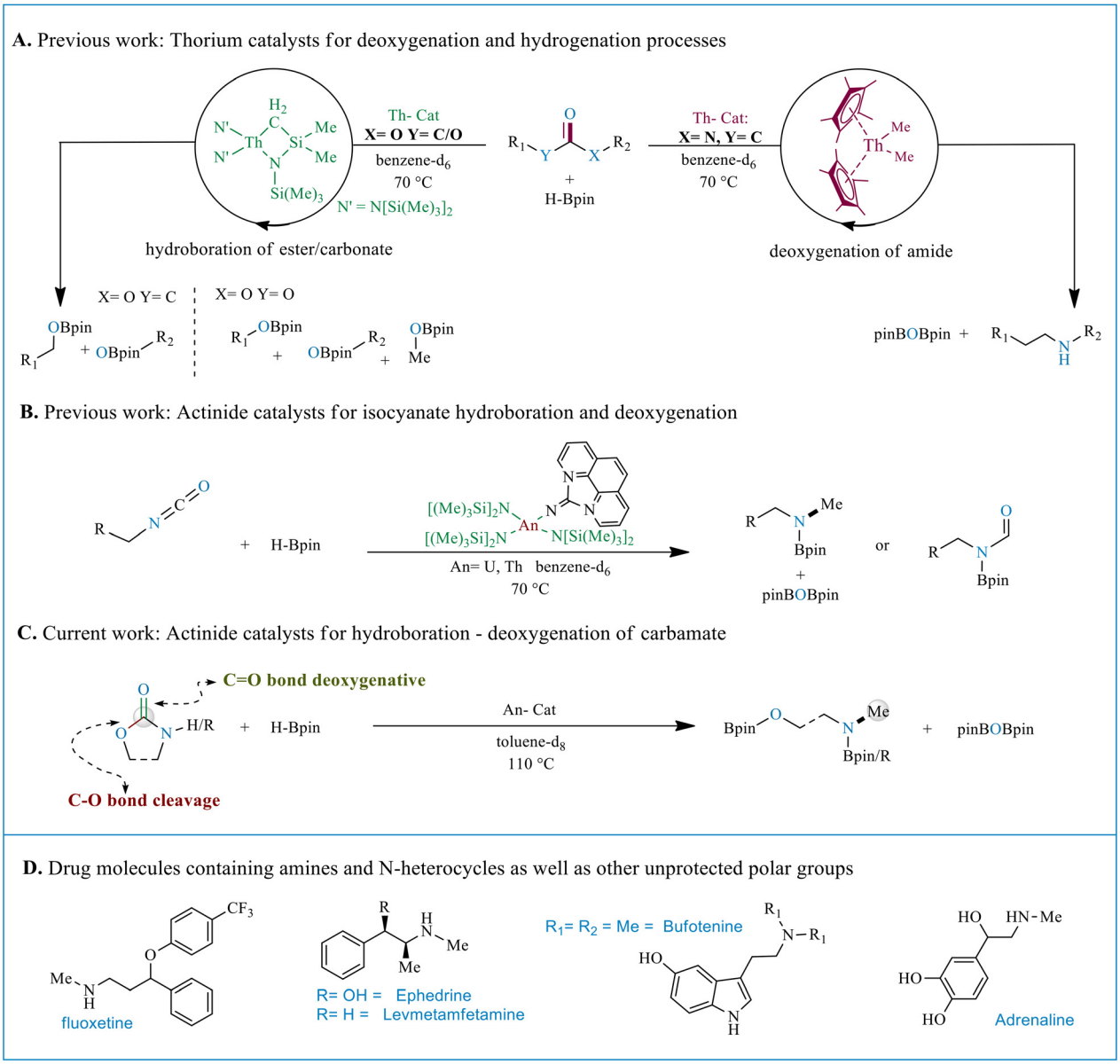

Fig. 1 (A) Previous work: thorium catalysts for deoxygenation and hydrogenation processes. (B) Previous work: actinide catalysts for isocyanate hydroboration and deoxygenation. (C) Current work: actinide catalysts for hydroboration–deoxygenation of carbamate. (D) Drug molecules containing alkylamines, N-heterocycles, and other polar groups.

isocyanates toward *N*-methylamines through the formation of formamide intermediates *via* C═N bond reduction, followed by deoxygenation (Fig. 1B).[31] To the best of our knowledge, the use of organo-f-complexes to activate carbamates has not been reported. In this regard, the catalytic activity and mode of action of the organo-f-complexes in this area are interesting, particularly for enhanced selectivity and reactivity to either multifunctional or stable carbamates, including polymers and bioactive molecules. To this end, based on the previous ester, carbonate, isocyanate, and amide protocols,[28–31] activating carbamates (Fig. 1C), will display recycling a hydride, An–H, from the corresponding oxide, An–O, *via* a C–O bond cleavage as in esters or carbonates, and the C═O deoxygenation as in amides and isocyanates, which eventually will streamline the catalytic activation of carbamates. It will provide direct access to the synthesis of valuable, multi-functional moieties, such as amino alcohols, *N*-methylamines, and tertiary alkylamines, using carbamates as a promising feedstock. Moreover, the carbamate moiety and its corresponding deoxygenative bond cleavage products are also widely present in natural products, pharmaceuticals, and polymers.[32–37] However, its reduction using reagents such as $LiAlH_4$ often lacks selectivity.[38,39] Therefore, a selective mode of activation of multi-functional carbamates, particularly drug molecules, is both required and desirable; this selective modification of drug molecules can be considered a powerful and attractive method for developing

and discovering new drug molecules.[36,37,40] The research presented here is also motivated by the potential use of carbamates to produce complex amines, amino alcohols, and methylamine products, a framework that exists in a large number of drug molecules (Fig. 1D), and has wide applications in catalysis.[36,37,40]

Results and discussion

The synthesis of the coordinative unsaturated An(IV) metallacycle complexes **I** and **II**, [An = Th (**I**); U (**II**)], which were previously reported by Andersen *et al.*, was accomplished by treating the corresponding thorium or uranium tetrachloride with sodium bis(trimethylsilyl)-amide, which upon heating undergoes a γ-elimination of trimethylsilylamide forming the corresponding metallacycle An(IV) complexes **I** and **II**, as described in the literature.[41] The iminato thorium(IV) complex **III** was synthesized by a protonolysis between the corresponding neutral iminato ligand and the thorium(IV) metallacycle(I).[42,43] We initiated our investigations by examining the carbamate hydroboration and deoxygenation of 3-methyl-2-oxazolidinone (**1a**) as a model substrate to obtain the corresponding borylated *N*-methylaminol. We examine the catalytic activity of the three actinide complexes (**I–III**) with different hydride sources (Table 1). The reaction performed by complex **I** in THF and HBpin (**2**) did not yield any product, even after 48 hours (Table 1, entry 1), presumably due to the solvent's coordination towards the coordinatively unsaturated complexes, which inhibited the coordination and activation of the carbamate. The three actinide complexes (**I**, **II**, and **III**) exhibited low catalytic activities in the hydroboration of 3-methyl-2-oxazolidinone (**1a**) at 80 °C in benzene, yielding conversions of 20%, 16%, and 14%, respectively (Table 1, entries 2–4). The product of the reaction is formed after the reduction and deoxygenation of the C=O bond and the cleavage of the C–O Sigma bond to afford the corresponding borylated 2-dimethylaminoethanol (**1′a**) and bis(pinacolboryl)oxide (pinB-O-Bpin) as a coproduct. Interestingly, complex **I** exhibited high catalytic activity when toluene was used as a solvent at a higher temperature (110 °C), achieving a 72% conversion in 24 hours. Complexes **II** and **III** yielded conversions of 70% and 62%, respectively (Table 1, entries 5–7). The use of different hydride sources (Table 1, entries 8–11) demonstrated that HBpin and 9-BBN are effective hydride reagents for the hydroboration and the ring cleavage of the cyclic carbamate.

However, since we monitor the reactions by NMR, 9-BBN affords a complex spectrum as compared to HBpin, with broad multiple peaks in 9-BBN *versus* a sharp singlet in HBpin. Hence, we studied the substrate scope using HBpin and the three actinide complexes **I–III**. No reaction occurred in the absence of the actinide complexes (Table 1, entry 12).

Having established a viable protocol for the deoxygenation and hydroboration of carbamates, we explored the substrate scope of the general reaction (Fig. 2A). We started our scope studies with the protected cyclic carbamate 2-oxazolidinones

Table 1 Optimization of the reaction conditions for the carbamate activation, forming borylated 2-dimethylaminoethanol[a]

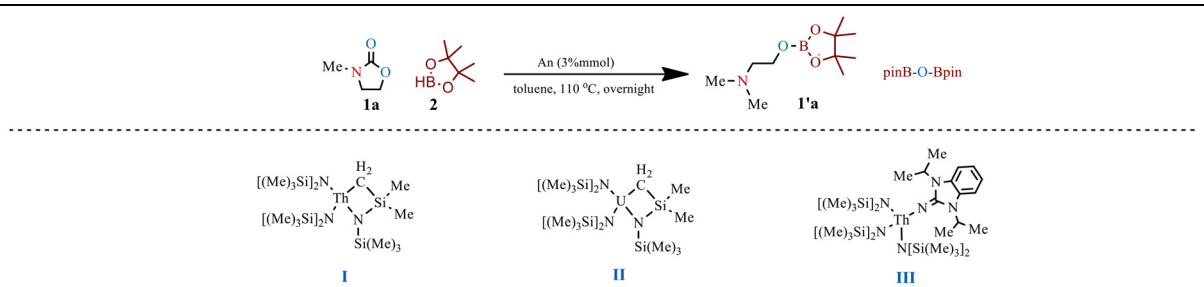

Entry	Catalyst [3%]	Solvent	H-source	Temp [°C]	Time [h]	Yield[b] [%]
1	**I**	THF	H-Bpin	66	48	—
2	**I**	Benzene	H-Bpin	80	24	20
3	**II**	Benzene	H-Bpin	80	24	16
4	**III**	Benzene	H-Bpin	80	24	14
5	**I**	Toluene	H-Bpin	110	24	72
6	**II**	Toluene	H-Bpin	110	24	70
7	**III**	Toluene	H-Bpin	110	24	62
8	**II**	Toluene	9-BBN	110	24	84
8	**II**	Toluene	BH_3*THF	110	24	8
9	**II**	Toluene	HBCat[c]	110	24	Traces
10	**II**	Toluene	$PhSiH_3$	110	24	13
11	**II**	Toluene	Et_3SiH	110	24	0
12	—	Toluene	H-Bpin	110	24	—

[a] Reaction conditions: 3-methyl-2-oxazolidinone (**1a**) (0.2 mmol), hydride source (0.63 mmol), An (mol 3%), solvent (0.65 mL), 110 °C and 24 h. [b] Yields were determined by ^{1}H NMR spectroscopy of the crude reaction mixture with an internal standard of hexamethylbenzene. [c] HBCat (catecholborane).

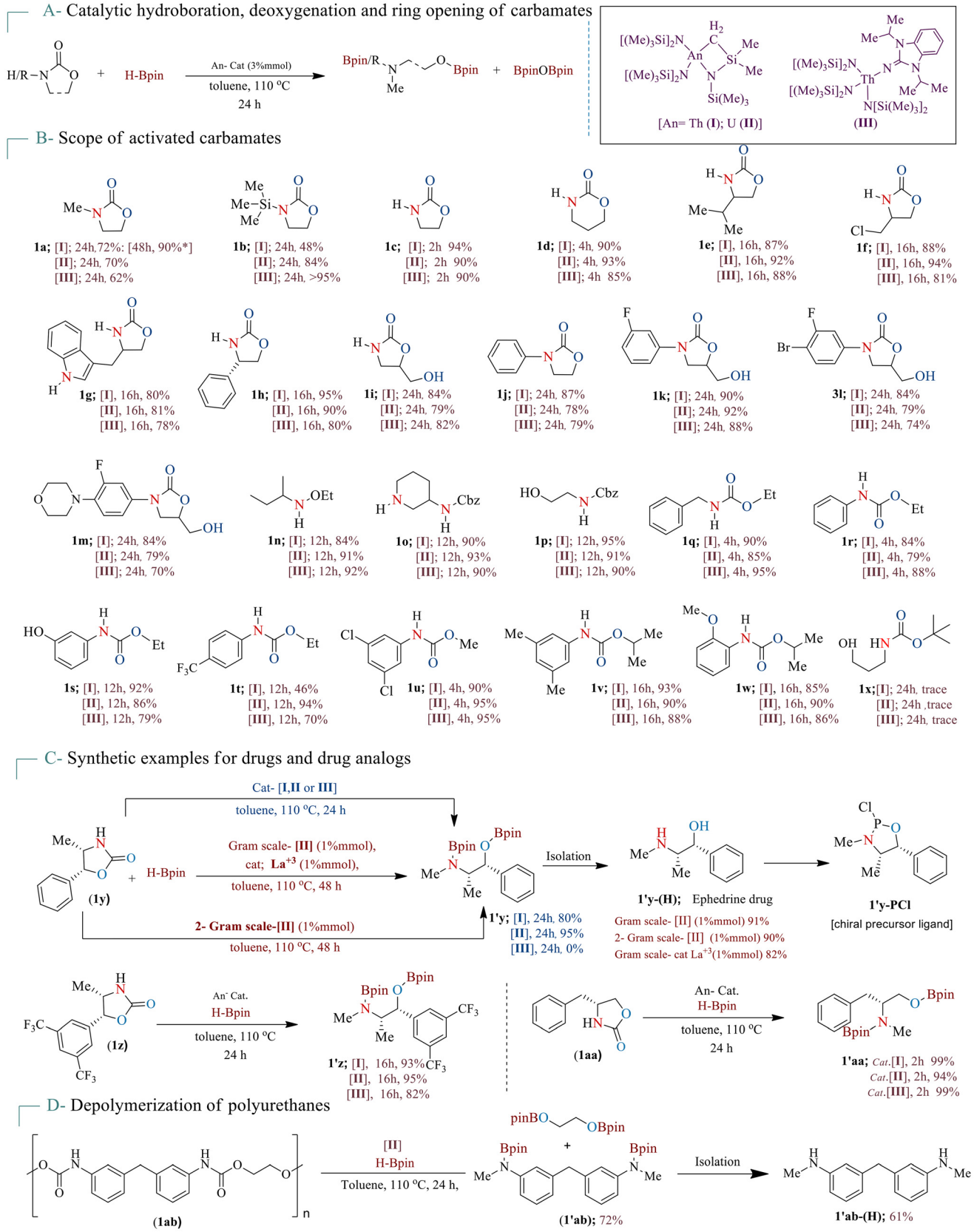

Fig. 2 Carbamate scope studies and details: (A) catalytic hydroboration, deoxygenation and ring opening of carbamates, (B) scope of activated carbamates, (C) synthetic examples for drugs and drug analogs, and (D) depolymerization of a polyurethane.

(Fig. 2B). First, the 3-methyl and 3-trimethylsilyl oxazolidinones (**1a** and **1b**) were studied, and the corresponding products were obtained in moderate to excellent NMR yields (50–95%) using complexes **I**, **II**, and **III** in 24 hours. In the case of the trimethylsilyl derivative (**1b**), the Th(IV) iminato complex **III** showed a better catalytic activity as compared with its Th(IV) metallacycle precursor **II**, 95% *vs.* 48%. Furthermore, a variety of free N–H cyclic carbamates were studied. 2-Oxazolidinones and 1,3-oxazinan-2-one (**1c** and **1d**) were effectively activated and achieved quantitative yields using the three complexes in only 2–4 hours, indicating that neither the ring size nor the free NH amido group inhibits the reactivity of the complexes. Next, we examined a set of different substitutions at the 2-oxazolidinones (**1e**, **1f**, **1g**, and **1h**), and it was found that our catalysts **I–III** effectively activated the carbamates towards the corresponding 1,3-aminoalcohols in good to excellent NMR yields, ranging from 72% to 95%, in an overnight reaction. For substrate **1h**, the chirality of the substrate remains unaffected. Interestingly, these actinide catalysts were also active with the 2-oxazolidinone containing a primary alcohol derivative (**1i**), which was converted to the corresponding borylated aminoalcohol, reaching excellent yields up to 84% in 24 h, illustrating that the hydroxyl group does not have a major effect on the catalytic activity of these actinide complexes under the reaction conditions. Hence, a variety of *N*-phenyl-protected 5-(hydroxymethyl)-3-phenyloxazolidin-2-one carbamates (**1j**, **1k**, **1l**, and **1m**) were studied, showing a small effect on the reactivity of the three catalysts, with conversions ranging from 70% to 92% in 24 hours. Moreover, the reactivity of different ethylamide-carbamate (**1n**) or benzyloxycarbonyl Cbz-aliphatic carbamates (**1o** and **1p**) was found to be similar to the reactivity obtained with the 2-oxazolidinone derivatives with good to excellent yields (84%–95%) after 12 h. The reaction scope was next explored with a series of aromatic non-cyclic carbamates (**1q–1w**), featuring electron-withdrawing groups (*e.g.*, CF_3) and electron-donating groups (*e.g.*, Me), as well as different alkyl chains, yielding excellent results in 4–16 hours. Concerning the alkoxide OR chains, it was found that the bulkiness of the OR moiety significantly affects the catalytic reactivity. The carbamate with the O–Me group (**1u**) reached almost quantitative yield in 4 hours, while the corresponding isopropyl derivatives (**1v** and **1w**) achieved excellent yields only after 16 hours. Moreover, the *tert*-butyl aliphatic carbamate (**1x**) showed only trace conversions after 24 h. To highlight the synthetic potential of activating carbamates *via* their hydroboration, followed by deoxygenation and C–O cleavage to obtain the corresponding N–Me derivatives, we focused on investigating the potential ability to synthesize drug or drug analog molecules (Fig. 2C). In this regard, the use of the commercially available (4*S*,5*R*)-(−)-4-methyl-5-phenyl-2-oxazolidinone (**1y**) produces the corresponding borylated (−) ephedrine drug molecule **1′y** using the An(IV) metallacycles [An = Th (**I**); U (**II**)] in excellent yields of 80–95%, which also participates furthermore in ligand synthesis, providing the ligand precursor **1′yPCl**. Next, we explored the potential application of this protocol by performing gram and 2-gram-scale reactions. Delightfully, no substantial loss of the yield was noticed; the reaction delivered the (−) ephedrine drug molecule (**1′y-H**) after its isolation in excellent yields of 91% and 90% in 48 h, using a 1% mmol of the An(IV) metallacycle (**II**), instead of 3% mmol (Fig. 2C). Moreover, for synthetic application, we extend this gram-scale protocol using the commercially available La^{+3} complex [tris[*N*,*N*-bis(trimethylsilyl)amide]lanthanum(III)]. The lanthanide complex also showed excellent activity at 1% mmol, yielding the corresponding isolated (−) ephedrine.

The (−) ephedrine molecule **1′y-H** was obtained in 82% yield after 48 h, maintaining the chiral center intact (Fig. 2C). Next, a fluorinated ephedrine drug analog (**1′z**) was effectively produced in 93%, 95%, and 82% yields using catalysts [**I–III**], respectively, within 24 hours, using the commercially available fluorinated 4-methyl-5-phenyl-2-oxazolidinone (**1z**) substrate. In addition, the 4-benzyl-2-oxazolidinone (**1aa**) was effectively transformed into the methamphetamine drug analog **1′aa**, containing a hydroxyl group on the terminal carbon, by catalysts **I**, **II**, and **III** in 2 hours, reaching quantitative yields of 99%, 94%, and 99%, respectively (Fig. 2C). Another intriguing and challenging area is polymer recycling. Carbamate-based polymers are widely used in industry owing to their wide applications, which stem from their exceptional stability.[44–46] However, their stability makes them difficult to recycle or even transform. As a result, the depolymerization of polyurethanes to manufacture high-value chemicals, *e.g.*, methylamine-containing compounds, has remained unachievable under the conditions of a homogeneous catalytic protocol.[47–49] Therefore, we focused on investigating the potential ability of the actinide complexes to activate polyurethanes (Fig. 2D). Subsequently, the addition of HBpin to a polyurethane (**1ab**) in the presence of 3% mmol of the uranium catalyst (**II**) results in its depolymerization and its conversion into the borylated dimethyldiaminodiphenylmethane (**1′ab**) and the borylated ethylene glycol with good yields (74%) in 24 h, providing a facile catalytic route for a controlled polymer degradation. A simple silica-gel purification of the borylated compound **1′ab**, yielded the corresponding hydrolyzed free N–H dimethyldiaminodiphenylmethane (**1′ab-H**), which was isolated in good yield (61%). It is worth mentioning that this protocol presents, for the first time, the homogeneous transformation of a polyurethane into a methylamine framework. It is well known that organic synthesis remains the rate-limiting factor in drug discovery despite decades of groundbreaking research in academia.[33] In this regard, a late-stage modification or functionalization signifies a valuable methodology for rapidly constructing novel analogs of drug molecules and pharmaceutically active agents. Therefore, to highlight the applicability of this protocol, we evaluated the carbamate activation methodology (hydroboration followed by deoxygenation, ring opening for cyclic carbamates, and protonolysis during the purification) with biologically active compounds and natural products (Fig. 3). As shown in Fig. 3, the current strategy provides practical evidence for the late stage deoxygenative hydroboration of various biologically active carbamate compounds, including commercial pharmaceuticals. The modified scope

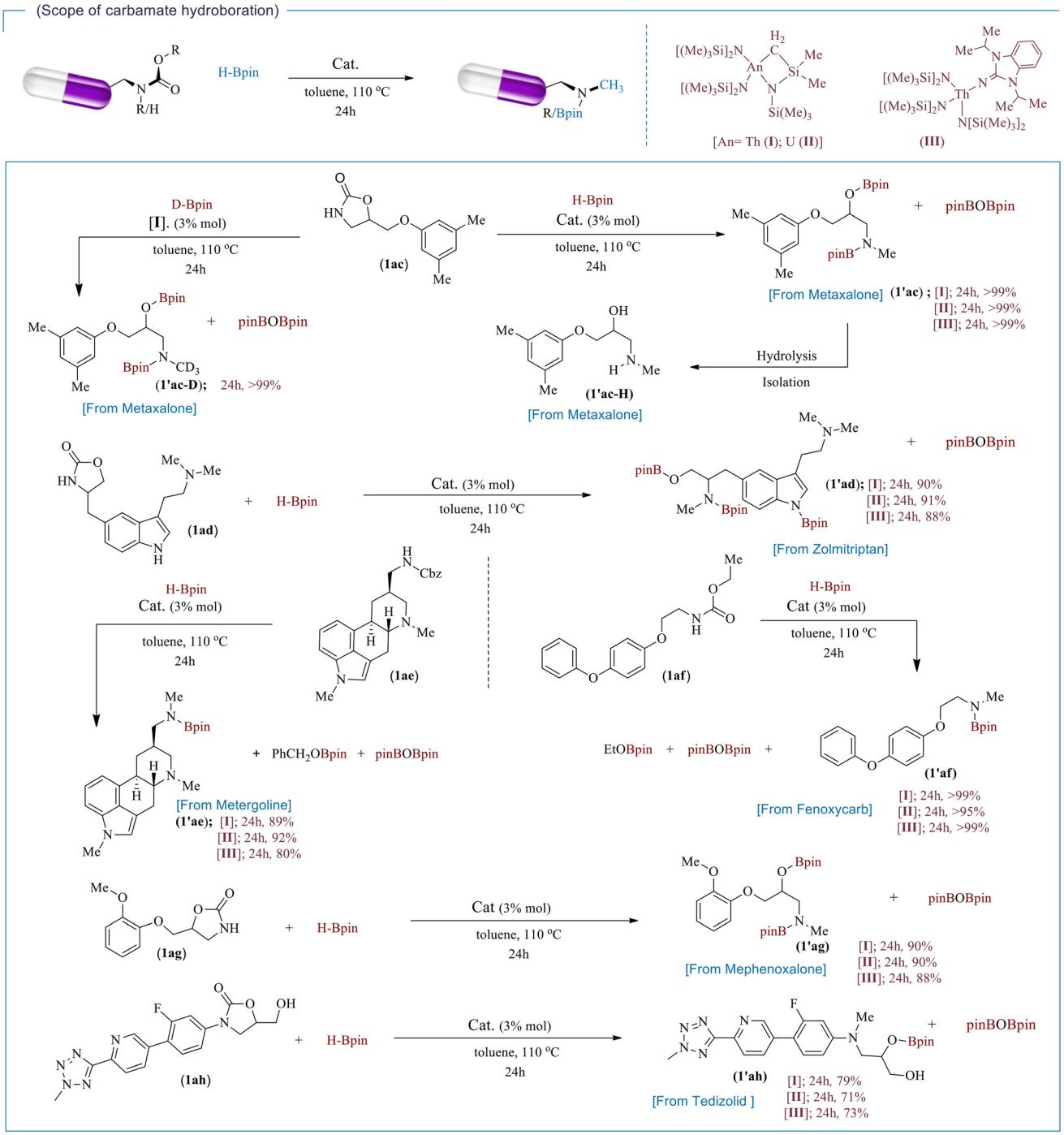

Fig. 3 Carbamate hydroboration for late-stage modification of drug molecules and pharmaceutically active agents.

was studied by investigating the drug metaxalone (**1ac**). Metaxalone effectively underwent hydroboration, ring opening and deoxygenation towards the diborylated 1-(3,5-dimethylphenoxy)-3-(methylamino)propan-2-ol **1′ac**, with quantitative conversion (>99%) in 24 h using any of the three catalysts studied (**I–III**). The hydrolysis of the diborylated **1′ac** yields the corresponding 1-(3,5-dimethylphenoxy)-3-(methylamino) propan-2-ol (**1ac-H**) in 81% isolated yield. The incorporation of the *N*-trideuteromethyl group into pharmaceuticals has been shown to enhance their metabolic stability.[50] Hence, metaxalone transformation was performed using D-Bpin, displaying a similar reactivity to HBpin. The corresponding diborylated, deuterated and modified 1-(3,5-dimethylphenoxy)-3-((methyl-d_3)amino)propan-2-ol (**1′ac-D**) was obtained in quantitative D-incorporation yields after 24 h using complex **I**.

Next, the drug zolmitriptan (**1ad**) efficiently participated in this process, affording the biologically interesting products (**1′ad**) in excellent yields (88%–91%) in 24 h using the three cata-

lysts (**I**, **II**, and **III**). It is worth mentioning that the modified zolmitriptan drug product (**1′ad**) is highly similar to sumatriptan and relatively similar to rizatriptan and almotriptan, which are other triptan drug molecules. A late-stage modification was also explored using the bioactive drugs metergoline (**1ae**) and fenoxycarb (**1af**). Both were hydroborated and deoxygenated with C–O cleavage, yielding the corresponding modified molecules (**1′ae** and **1′af**) smoothly in 24 hours with excellent yields of up to 92% and 99% for metergoline and fenoxycarb, respectively, using the three complexes **I–III**.

In addition, the drug mephenoxalone (**1ag**) was successfully modified to the corresponding product (**1′ag**) in 24 h in excellent yield (~90%). Interestingly, the mephenoxalone modified product (**1′ag**) is highly similar to the bioactive molecules, guaifenesin, moprolol, and methocarbamol. Lastly, the drug tedizolid (**1ah**) was efficiently modified using this protocol, reaching 71–79% of the corresponding products (**1′ah**) in 24 h using the actinide complexes as presented in Fig. 3.

Kinetic and thermodynamic studies for the carbamate hydroboration, deoxygenation, and ring opening *via* a C–O cleavage

Kinetic studies for the catalytic hydroboration of 3-methyl-2-oxazolidinone (**1a**) employing the uranium catalyst (**II**) were conducted by changing one of the substrates or the catalyst while keeping the other reagents in excess and constant. The progress of the reaction was monitored *via in situ* ^{1}H NMR spectroscopy. The rate of the product formation displays a first-order dependence on the uranium catalyst (**II**), a first-order dependence on HBpin, and a zero-order dependence on 3-methyl-2-oxazolidinone (**1a**), giving rise to the kinetic eqn (1)

$$\frac{\partial p}{\partial t} = K_{(\mathrm{obs})} \cdot [\mathbf{II}]^1[\mathrm{HBpin}]^1[\mathrm{carbamate}]^0. \quad (1)$$

The activation thermodynamic parameters were calculated from the Eyring and Arrhenius plots over the temperature range of 70–120 °C, displaying an energy of activation (E_a) of 8.46 ± 0.11 kcal mol^{-1}, an enthalpy of activation ($\Delta H^{\ddagger}$) of 7.73 ± 0.11 kcal mol^{-1}, and a large negative entropy of activation ($\Delta S^{\ddagger}$) of −55.9 ± 3.0 eu. The $\Delta S^{\ddagger}$ data are consistent with a simultaneous bond-cleavage and bond-formation event with a very organized four-membered ring at the rate-determining step.

Competitive experiments and mechanistic studies in the carbamate hydroboration, deoxygenation, and ring opening *via* C–O cleavage

To further investigate the selectivity of the catalytic activation of carbamates, we conducted competitive experiments using catalyst **II** on the carbamate functionality, along with other functional groups that could potentially be activated in the presence of an actinide-based catalyst (Fig. 4). We initiated the examination by comparing the protecting carbamate 3-methyl-2-oxazolidinone (**1a**) (0.2 mmol) with ethylene carbonate (0.2 mmol) using 0.6 mmol of HBpin. As expected, the chemoselective activation of the carbonate produced the diborylated ethylene glycol and the borylated methanol, while the substrate 3-methyl 2-oxazolidinone (**1a**) remained unreacted.

The same reactivity was observed when equimolar amounts of the carbamate and benzyl-formamide (0.2 mmol) were activated at the same time, producing only the *N*-methylbenzylamine and the diborane pinBOBpin, keeping the carbamate intact. This reactivity is attributed to the reactive nature of the different carbonyl groups. Hence, a subsequent competitive experiment was conducted between equimolar amounts of 3-methyl-2-oxazolidinone (**1a**) and the corresponding unprotected 2-oxazolidinone (**1c**) (0.2 mmol). As expected, the activation occurred on the 2-oxazolidinone (**1c**) due to the difference in electronic effects between the two substrates (*vide infra*). Competition between 2-oxazolidinones (**1c**) and benzylformamide is more intriguing. The competition hydroboration between equimolar amounts of 2-oxazolidinones (**1c**) and benzylformamide using 0.6 mmol of HBpin resulted in the hydroboration of the benzylformamide with 67% conversion and the hydroboration of 2-oxazolidinones (**1c**) with a conversion of 48%. This suggests that formamide reacts faster than 2-oxazolidinones, even though it is a free N–H carbamate derivative. In a similar competitive reaction with a more reactive aldehyde functional group, PhCHO (0.2 mmol) was exclusively hydroborated. However, a competition reaction between 2-oxazolidinones (**1c**) (0.2 mmol) and the unsaturated alkene (0.2 mmol) or alkyne (0.2 mmol) provides a full hydroboration of the 2-oxazolidinones (**1c**). Interestingly, the same chemoselectivity towards the carbamate is observed when reacting 2-oxazolidinones (**1c**) with a pyridine or a nitrile substrate, keeping the latter ones unaffected.

To shed light on the catalytic process, stoichiometric reactions were performed to trap possible intermediates (Fig. 5). The model reaction (Fig. 5A) was catalyzed by complex **I** and monitored using ^{1}H NMR to gain mechanistic insight into the activation of this carbamate. The activation's first step involved forming complex **D** with an aldehydic signal [δ = 11.7 ppm], which supports the formation of a formamide during the reaction. Owing to its higher reactivity relative to the carbamate at the reaction temperature, only trace amounts were detected. Therefore, different formamide derivatives were efficiently hydroborated nearly quantitatively in 3 h (Fig. 5B). Deuterium-labeling experiments (Fig. 5C) demonstrated the formation of the *N*-deuterated methyl with quantitative D-incorporation (>99%), which illustrates that HBpin/DBpin serves as the hydride source. In addition, proton and boron NMR spectroscopy analysis and HRMS showed the formation of the byproduct bis(pinacolboryl) oxide (pinB-O-Bpin). Moreover, studies performed on the corresponding thiocarbamate (Fig. 5D) resulted in the formation of traces of the boronated 1,3-amino-alcohol product, indicating a similar desulfurization.

DFT studies

To fully understand the catalytic behavior of the Th(IV) metallacycle complex (**I**) in the 3-methyl-2-oxazolidinone (**1a**) activation, an in-depth theoretical study, based on density functional theory (DFT), was carried out (the optimized geometries

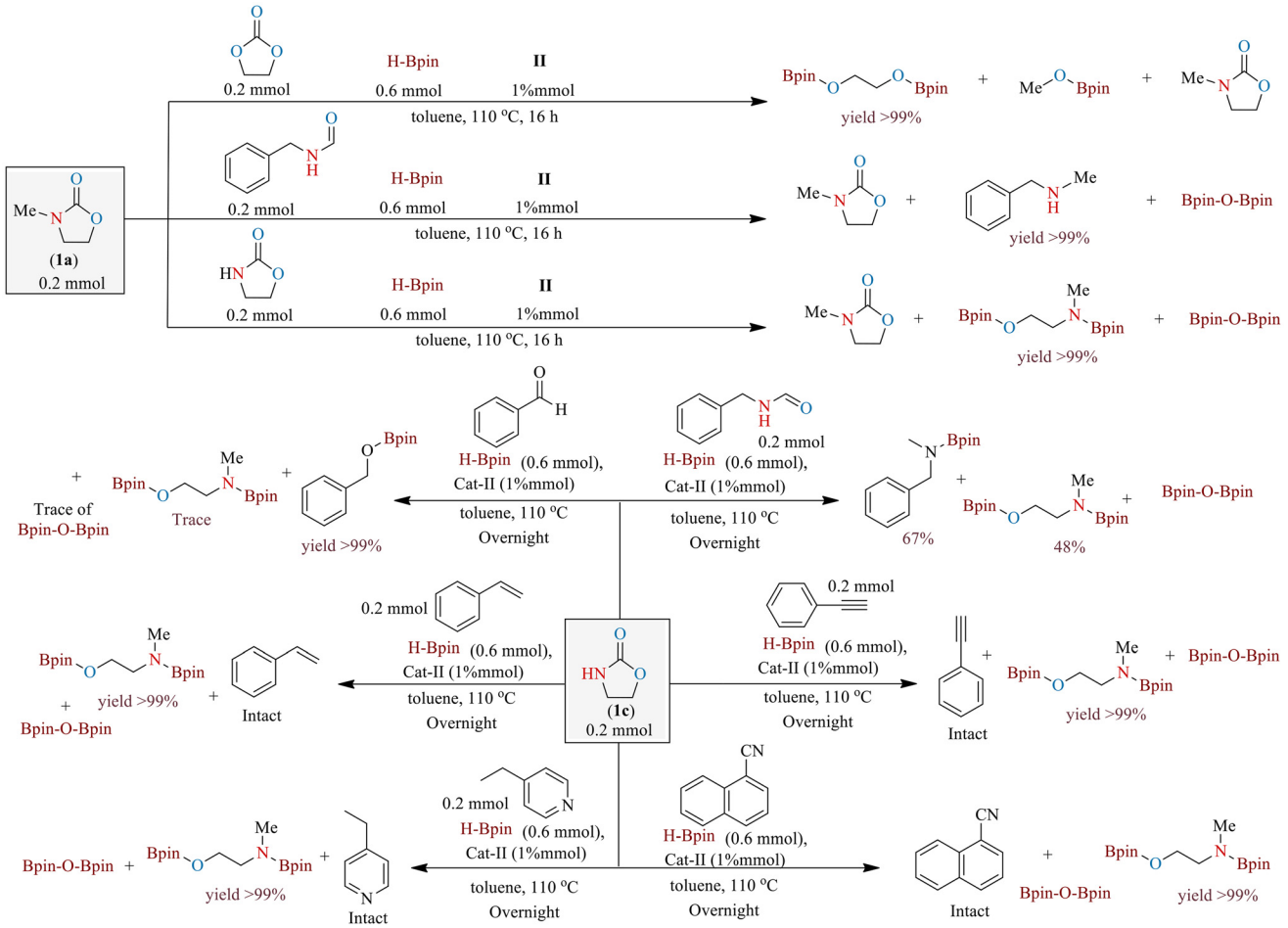

Fig. 4 Competitive activation of carbamates and substrates with additional functional groups by the uranium complex II.

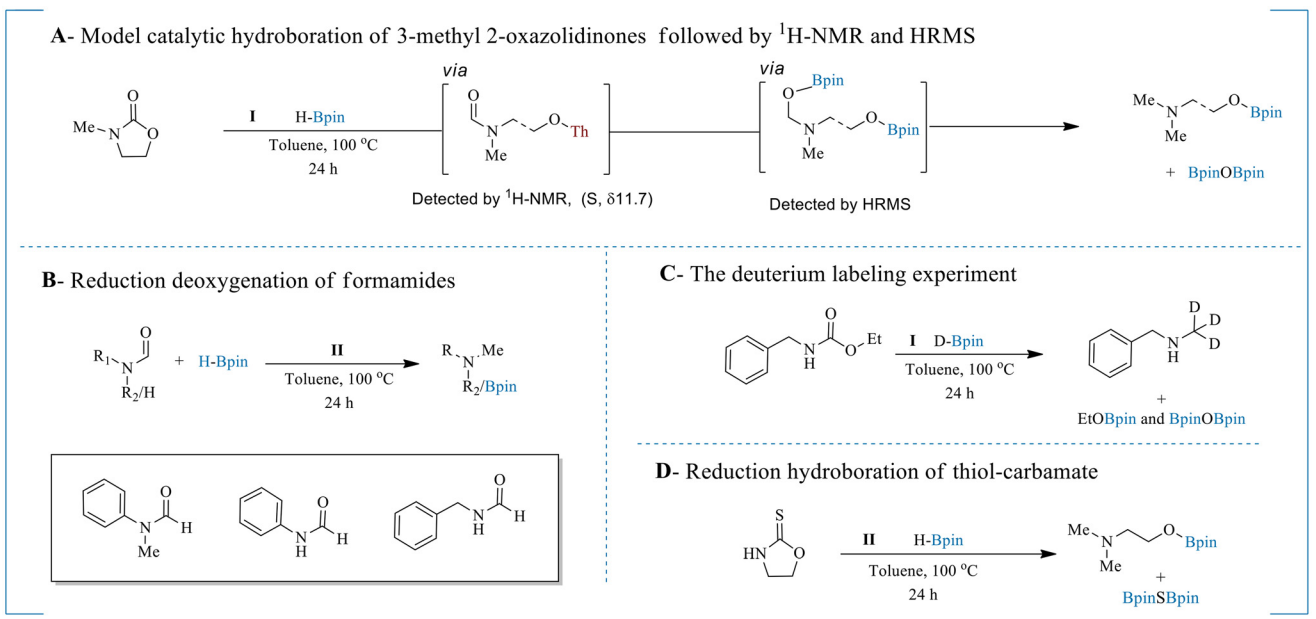

Fig. 5 (A) Model catalytic carbamate hydroboration monitored by ^{1}H-NMR, (B) reduction deoxygenation of formamides, (C) deuterium labelling experiment, and (D) reduction hydroboration of thiocarbamate.

of the transition states involved in the proposed catalytic mechanism are shown in Fig. S13 of the SI). The catalyst activation and the catalytic cycle reactions were thoroughly investigated, and the favored reaction pathways are discussed in detail below.

The proposed active catalyst is formed through the reaction between the Th(IV) metallacycle catalyst (**I**) and HBpin, which was set as the zero of the free energy, producing the actinide hydride (**A**″), at −9.6 kcal mol^{-1} below that of the catalyst (**I**), in which the boron atom of the Bpin fragment engages in an interaction with the hydride coordinated to the Th center. The opening of the four-membered metallacycle ring, involving Th–C and B–H bonds, occurs easily *via* TS-(**A**″) at 9.4 kcal mol^{-1}, leading to the formation of the Th–H bond in the intermediate (**A**″). The subsequent weakening of the B–H interaction and the rearrangement of the (Me_3Si)-N-Si$(Me)_2CH_2$-Bpin ligand led to the formation of the active species (**A**′), lying at only 0.3 kcal mol^{-1} from the reactants. To reduce computational costs, we performed the mechanistic study of the catalytic cycle using the truncated model (**A**). In this model, the (Me_3Si)-N-Si$(Me)_2CH_2$-Bpin ligand is replaced by a $(Me_3Si)_2N$ (N″) group, making it consistent with the other two ligands of the catalyst (Scheme 1).

The proposed catalytic cycle (Scheme 2) proceeds *via* the formation of the adduct (**B**), at −1.5 kcal mol^{-1} relative to the zero of the free energy, in which carbonyl oxygen of 3-methyl-2-oxazolidinone (**1a**) interacts with the metal center of the activated catalyst (**A**) (Scheme 2). From (**B**), the subsequent insertion of the carbamate C═O portion into the thorium hydride motif, *via* TS_1(**C**) at 7.0 kcal mol^{-1}, leads to the formation of the intermediate (**C**) at −27.8 kcal mol^{-1}, overcoming an energy barrier of only 8.5 kcal mol^{-1}.

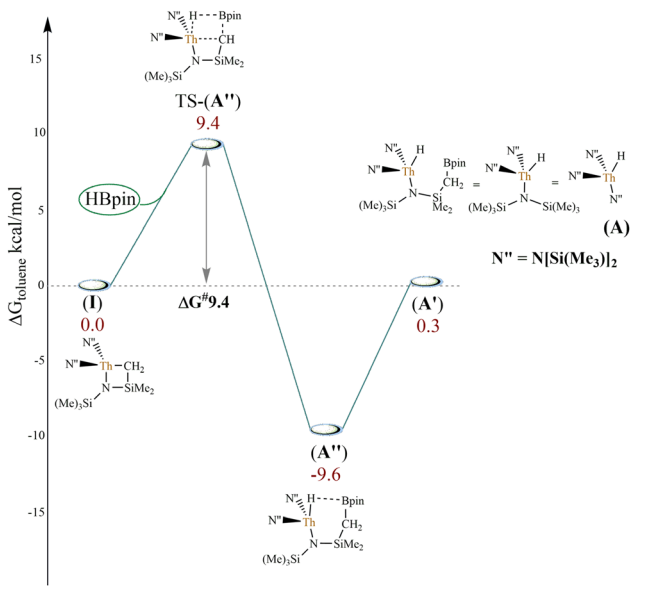

Scheme 1 DFT-computed energy profile related to the activation pathway of the Th metallacycle catalyst (**I**). The energy values are Δ*G* in kcal mol^{-1} in toluene as the solvent.

At this point, intermediate (**C**) undergoes a reorganization of the metal coordination sphere. Specifically, the thorium center shifts from the carbonyl oxygen of (**1a**) to the heterocyclic oxygen, yielding the more stable intermediate (**D**) at −42.4 kcal mol^{-1}. This transformation proceeds *via* transition state TS_2(**D**) with a calculated energy barrier of only 8.9 kcal mol^{-1}.

Starting from (**C**) we also investigated an alternative metathesis pathway involving a molecule of HBpin. However, the computed energy barrier was found to be approximately 10 kcal mol^{-1} higher than that of TS_2(**D**), and, consequently, this competitive route was ruled out.

From intermediate (**D**) a metathesis reaction occurs with the second molecule of HBpin (Scheme 2). This process involves the Th–O and H–B bonds and leads to the formation of intermediate (**E**) (at −31.3 kcal mol^{-1}). In this species, the regenerated active catalyst (**A**) interacts with the formamide product, $HC(O)N(CH_3)(CH_2)_2OBpin$. The transformation proceeds *via* transition state TS_3(**E**) at −24.2 kcal mol^{-1}, with a calculated energy barrier of 18.2 kcal mol^{-1} (Scheme 2). The reaction subsequently proceeds through the insertion of the formamide carbonyl group into the Th–H bond *via* TS_4(**F**) (−14.0 kcal mol^{-1}), yielding intermediate (**F**) at −55.1 kcal mol^{-1}. This transformation, calculated relative to the most stable species (**D**), entails an overall energy barrier of 28.4 kcal mol^{-1}.

These findings are in good agreement with the experimental results obtained from the stoichiometric reaction of 3-methyl-2-oxazolidinone (**1a**) with catalyst (**I**) in the presence of two equivalents of HBpin, which yields the corresponding formamide species.

Starting from (**D**), we also investigated an alternative pathway in which the Bpin moiety of a second HBpin molecule coordinates to the formamide carbonyl oxygen, followed by a concerted hydride transfer to the carbonyl carbon. However, this mechanism entails an energy barrier approximately 13 kcal mol^{-1} higher than that of TS_3(**E**) (Scheme 2). Consequently, this route was excluded from further considerations.

From (**F**), subsequent metathesis reaction, involving the Th–O bond and the H–B bond of a third HBpin molecule, affords intermediate (**G**) at −43.2 kcal mol^{-1}, regenerating the active catalyst (**A**) that interacts with the reaction product $pinBOCH_2N(CH_3)(CH_2)_2OBpin$. The transition state associated with the formation of (**G**), TS_5(**G**), lies at −31.2 kcal mol^{-1}, requiring an energy barrier of 23.9 kcal mol^{-1} (Scheme 2).

From (**G**), the borylated 2-dimethylaminoethanol (**1′a**), lying at −90.4 kcal mol^{-1}, is generated through an additional metathesis reaction between the O–Bpin bond of intermediate (**G**) and the thorium hydride motif of the active catalyst (**A**) *via* the TS_6(**1′a**) at −32.4 kcal mol^{-1}. The energy required for the final product formation (**1′a**), calculated relatively to intermediate (**F**), amounts to 22.7 kcal mol^{-1}.

Analysis of the complete energy profile for the deoxygenation of (**1a**) reveals that the conversion of (**D**) to (**F**) exhibits the highest overall energy barrier (28.4 kcal mol^{-1}), identifying

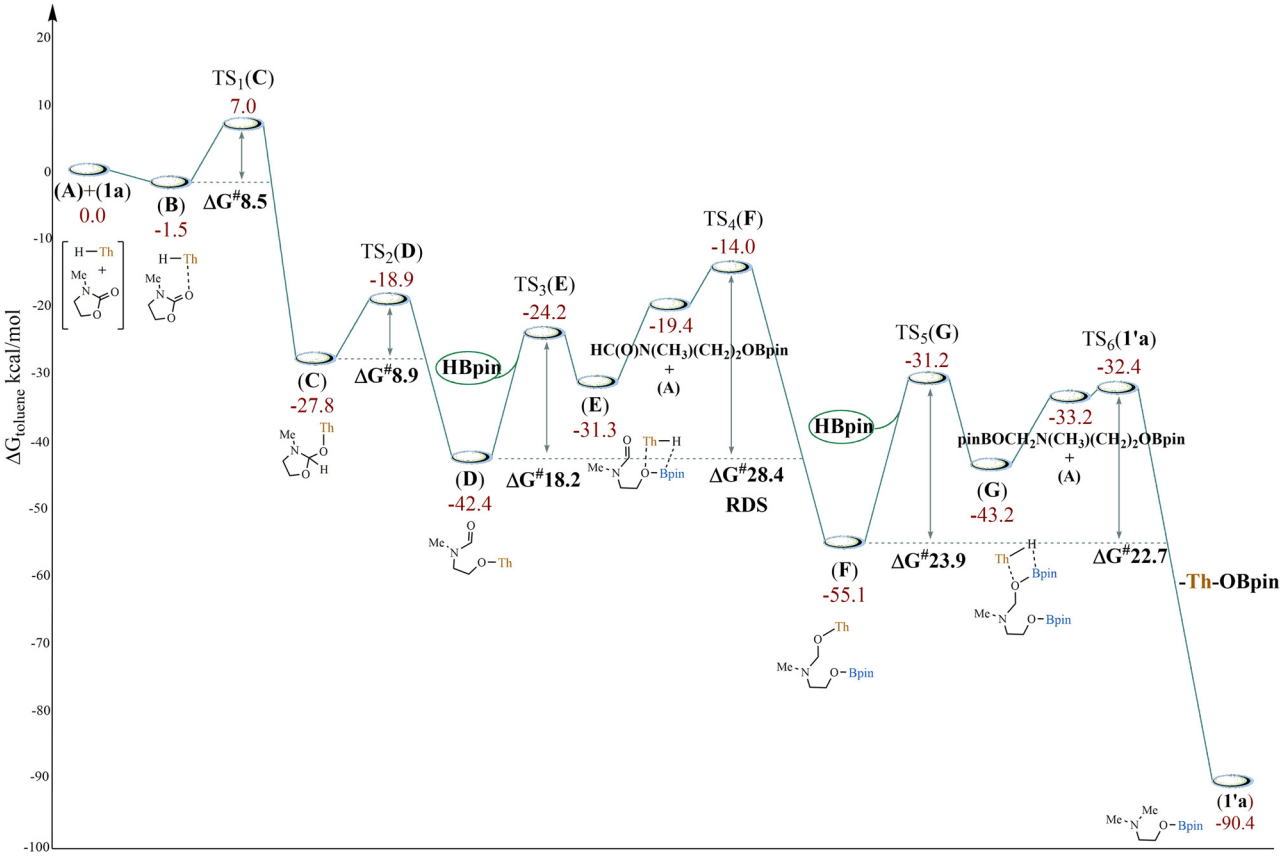

Scheme 2 DFT-computed energy for the C–O cleavage and C=O deoxygenation of the cyclic carbamate **1a** with HBpin catalyzed by the active thorium complex (**A**). The energy values are ΔG in kcal mol^{-1} in toluene as the solvent.

TS_4(**F**) as the rate-determining state for the entire catalytic cycle.

This result is consistent with the experimental kinetic studies reported for the analogous reaction catalyzed by uranium, showing a first-order dependence of the reaction rate on both the catalyst and HBpin concentrations with an experimental $\Delta G^{\ddagger}$ between 26.9 and 29.7 kcal mol^{-1} over the temperature range of 70–120 °C.

Based on the above analysis, a possible mechanism for the carbamate activation catalyzed by a thorium complex is presented in Fig. 6. The reactive Th–hydride complex (Th–H) (**A**) is generated *via* the cleavage of the Th–CH_2 bond in the Th(IV) metallacycle using HBpin.[30] Subsequent insertion of the carbamate into the Th–H bond leads to the formation of the Th-alkoxide intermediate (**C**). At this stage, a rearrangement of the metal coordination environment of (**C**) occurs, resulting in the cleavage of the carbamate σ(C–O) bond and the formation of the formamide intermediate (**D**). Subsequent σ-bond metathesis of the Th–O bond in (**D**), mediated by HBpin, regenerates the thorium hydride (**A**) to yield the borylated formamide intermediate (HC(O)N$(CH_3)(CH_2)_2$OBpin), which remains coordinated to the metal center in the transient adduct (**E**). Insertion of (**E**) into Th–H bond results in the reduction of the C=O double bond and forms the Th-alkoxide intermediate (**F**).

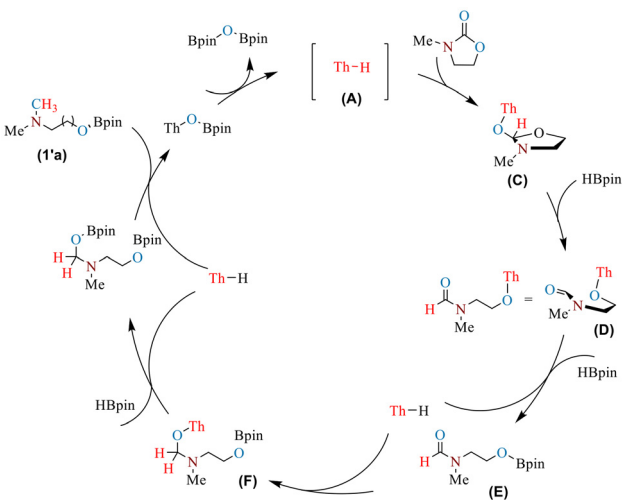

Fig. 6 Proposed mechanism for the hydroboration of carbamates catalyzed by thorium complexes.

Further metathesis of the Th–O bond in (**F**) with an HBpin produces the double borylated diol amine intermediate BpinOCH$_2$N$(CH_3)(CH_2)_2$OBpin with the concomitant regeneration of the Th–H species (**A**). The metathesis of the borylated diol

amine with (**A**) produces the product (**1′a**) and a Th–O–Bpin species, which reacts with another HBpin releasing the additional product, bis(pinacolato)diboron oxide (pinB–O–Bpin), and regenerates the active catalyst (**A**), completing the catalytic cycle.

Conclusions

In summary, An(IV) metallacycle/iminato complexes [An = Th, U] exhibit notable capabilities in activating carbamate molecules. Their efficacy as a homogeneous catalyst for the activation, deoxygenation, and bond cleavage of carbamate derivatives is reported here. The catalytic activities have demonstrated remarkable efficiency in direct deoxygenation and selective bond cleavage, reducing C═O bonds and cleaving C–O bonds, thereby producing the corresponding borated amino alcohol and trialkyl amine compounds. A broad scope of carbamates was converted into various amines and amino alcohols. Highlighting the potential applicability of carbamates, (−) ephedrine, ephedrine fluorinated analog, and others were obtained from the corresponding carbamate compounds. An (IV) metallacycle and iminato complexes were also found to be active against more complex molecules, demonstrating the potential for late-stage modification of different carbamate drug molecules and leading to interesting biological products. The modification occurs *via* a selective activation mode toward the carbamate, leaving the rest of the molecules intact, underscoring the potential of actinides/lanthanides as innovative catalysts and paving the way for more efficient and valuable methods for amine synthesis in organic chemistry. Moreover, this protocol is presented for the first time as a polymer-recycling approach for polyurethanes to *N*-methylamine compounds, in a homogeneous catalytic reaction that is highly sought after in research and industry, as recycling is complicated by the stability of polyurethanes. Kinetic studies displayed a rate law with a first-order dependence on the catalyst and pinacol borane (HBpin), and a zero-order dependence on the carbamate concentration. In addition, different stoichiometric experiments were performed, including deuterated labelling, competition reactions, and a combination with DFT computational methods, allowing us to provide a mechanism for this transformation. Further examination of the chemo- and regio-selectivity of this unusual catalytic reactivity and its application toward introducing new transformations is in progress and will be reported in the future.

Author contributions

T. S. conducted the experiments, synthesized the complexes, developed the substrate scope, and carried out detailed mechanistic studies, including kinetic experiments and thermodynamic measurements. I. R. designed and performed the DFT calculations. All authors wrote the manuscript. All authors commented on the final draft and contributed to the analysis and interpretation of the data.

Conflicts of interest

The authors declare no competing financial interest.

Data availability

The supporting data for this manuscript have been provided fully in the supplementary information (SI). Supplementary information: materials, methods and general remarks, procedures and characterization of all the compounds; stoichiometric reactions; large scale reactions; kinetics details, NMR spectra for all compounds; formaldehyde experiments; and computational details. See DOI: **https://doi.org/10.1039/d6qi00325g**.

Acknowledgements

This work was supported by the PAZY Foundation Fund (ID 843-2026), administered by the Israel Atomic Energy Commission. T. S. is grateful for a Ph.D. fellowship from the Neubauer Foundation and the Schulich Faculty of Chemistry, Technion-Israel Institute of Technology. L. C. acknowledges the Italian MUR for funding through the PRIN2022 project "Matisse" (No. 2022K5SX27).

References

1 J. Leduc, M. Frank, L. Jürgensen, D. Graf, A. Raauf and S. Mathur, Chemistry of Actinide Centers in Heterogeneous Catalytic Transformations of Small Molecules, *ACS Catal.*, 2019, **9**, 4719–4741.
2 J. Du, C. Alvarez-Lamsfus, E. P. Wildman, A. J. Wooles, L. Maron and S. T. Liddle, Thorium-Nitrogen Multiple Bonds Provide Evidence for Pushing-from-below for Early Actinides, *Nat. Commun.*, 2019, **10**, 4203.
3 T. W. Hayton, Metal-Ligand Multiple Bonding in Uranium: Structure and Reactivity, *Dalton Trans.*, 2010, **39**, 1145–1158.
4 A. R. Fox, S. C. Bart, K. Meyer and C. C. Cummins, Towards Uranium Catalysts, *Nature*, 2008, **455**, 341–349.
5 S. T. Liddle, The Renaissance of Non-Aqueous Uranium Chemistry, *Angew. Chem.*, 2015, **127**, 8726–8764.
6 T. Andrea and M. S. Eisen, Recent Advances in Organothorium and Organouranium Catalysis, *Chem. Soc. Rev.*, 2008, **37**, 550–567.
7 S. M. Mansell, N. Kaltsoyannis and P. L. Arnold, Small Molecule Activation by Uranium Tris(Aryloxides): Experimental and Computational Studies of Binding of N2, Coupling of CO, and Deoxygenation Insertion of CO_2 under Ambient Conditions, *J. Am. Chem. Soc.*, 2011, **133**, 9036–9051.
8 P. L. Arnold, T. Ochiai, F. Y. T. Lam, R. P. Kelly, M. L. Seymour and L. Maron, Metallacyclic Actinide Catalysts for Dinitrogen Conversion to Ammonia and Secondary Amines, *Nat. Chem.*, 2020, **12**, 654–659.

9 A. N. Price, V. Berryman, T. Ochiai, J. J. Shephard, S. Parsons, N. Kaltsoyannis and P. L. Arnold, Contrasting Behaviour under Pressure Reveals the Reasons for Pyramidalization in Tris(Amido)Uranium(III) and Tris (Arylthiolate) Uranium(III) Molecules, *Nat. Commun.*, 2022, **13**, 3931.
10 F. C. Hsueh, L. Barluzzi, M. Keener, T. Rajeshkumar, L. Maron, R. Scopelliti and M. Mazzanti, Reactivity of Multimetallic Thorium Nitrides Generated by Reduction of Thorium Azides, *J. Am. Chem. Soc.*, 2022, **144**, 3222–3232.
11 N. Jori, L. Barluzzi, I. Douair, L. Maron, F. Fadaei-Tirani, I. Živković and M. Mazzanti, Stepwise Reduction of Dinitrogen by a Uranium-Potassium Complex Yielding a U(VI)/U(IV) Tetranitride Cluster, *J. Am. Chem. Soc.*, 2021, **143**, 11225–11234.
12 B. M. Gardner and S. T. Liddle, Small-Molecule Activation at Uranium(III), *Eur. J. Inorg. Chem.*, 2013, **2013**, 3753–3770.
13 P. L. Arnold, T. Ochiai, F. Y. T. Lam, R. P. Kelly, M. L. Seymour and L. Maron, Metallacyclic Actinide Catalysts for Dinitrogen Conversion to Ammonia and Secondary Amines, *Nat. Chem.*, 2020, **12**, 654–659.
14 D. J. Grant, T. J. Stewart, R. Bau, K. A. Miller, S. A. Mason, M. Gutmann, G. J. McIntyre, L. Gagliardi and W. J. Evans, Uranium and Thorium Hydride Complexes as Multielectron Reductants: A Combined Neutron Diffraction and Quantum Chemical Study, *Inorg. Chem.*, 2012, **51**, 3613–3624.
15 S. T. Liddle, Progress in Nonaqueous Molecular Uranium Chemistry: Where to Next?, *Inorg. Chem.*, 2024, **63**, 9366–9384.
16 M. Keener, L. Maria and M. Mazzanti, Progress in the Chemistry of Molecular Actinide-Nitride Compounds, *Chem. Sci.*, 2023, **14**, 6493–6521.
17 E. J. Coughlin, Y. Qiao, E. Lapsheva, M. Zeller, E. J. Schelter and S. C. Bart, Uranyl Functionalization Mediated by Redox-Active Ligands: Generation of O-C Bonds via Acylation, *J. Am. Chem. Soc.*, 2019, **141**, 1016–1026.
18 S. Wang, Y. Heng, T. Li, D. Wang, G. Hou, G. Zi and M. D. Walter, Intrinsic Reactivity of [H5-1,3-$(Me_3Si)_2C_5H_3]_2U(H_4$-$C_4Ph_2)$ in Small Molecule Activation, *Dalton Trans.*, 2022, **51**, 11072–11085.
19 J. M. Berg, D. L. Clark, J. C. Huffman, D. E. Morris, A. P. Sattelberger, W. E. Streib, W. G. Van Der Sluys and J. G. Watkin, Early Actinide Alkoxide Chemistry. Synthesis, Characterization, and Molecular Structures of Th(IV) and U(IV) Aryloxide Complexes, *J. Am. Chem. Soc.*, 1992, **114**, 10811–10821.
20 T. Ghatak, K. Makarov, N. Fridman and M. S. Eisen, Catalytic Regeneration of a Th-H Bond from a Th-O Bond through a Mild and Chemoselective Carbonyl Hydroboration, *Chem. Commun.*, 2018, **54**, 11001–11004.
21 E. Balaraman, C. Gunanathan, J. Zhang, L. J. W. Shimon and D. Milstein, Efficient Hydrogenation of Organic Carbonates, Carbamates and Formates Indicates Alternative Routes to Methanol Based on CO_2 and CO, *Nat. Chem.*, 2011, **3**, 609–614.
22 E. Balaraman, Y. Ben-David and D. Milstein, Unprecedented Catalytic Hydrogenation of Urea Derivatives to Amines and Methanol, *Angew. Chem., Int. Ed.*, 2011, **50**, 11702–11705.
23 J. Pritchard, G. A. Filonenko, R. Van Putten, E. J. M. Hensen and E. A. Pidko, Heterogeneous and Homogeneous Catalysis for the Hydrogenation of Carboxylic Acid Derivatives: History, Advances and Future Directions, *Chem. Soc. Rev.*, 2015, **44**, 3808–3833.
24 G. Sai Kumar, J. Bhattacharjee, K. Kumari, S. Moorthy, A. Bandyopadhyay, S. Kumar Singh and T. K. Panda, Hydroboration of Nitriles, Esters, and Amides Catalyzed by Simple Neosilyllithium, *Polyhedron*, 2022, **219**, 115784.
25 M. K. Barman, A. Baishya and S. Nembenna, Magnesium Amide Catalyzed Selective Hydroboration of Esters, *Dalton Trans.*, 2017, **46**, 4152–4156.
26 X. Cao, W. Wang, K. Lu, W. Yao, F. Xue and M. Ma, Magnesium-Catalyzed Hydroboration of Organic Carbonates, Carbon Dioxide and Esters, *Dalton Trans.*, 2020, **49**, 2776–2780.
27 T. Iwasaki and K. Nozaki, Counterintuitive Chemoselectivity in the Reduction of Carbonyl Compounds, *Nat. Rev. Chem.*, 2024, **8**, 518–534.
28 S. Saha and M. S. Eisen, Mild Catalytic Deoxygenation of Amides Promoted by Thorium Metallocene, *Dalton Trans.*, 2020, **49**, 12835–12841.
29 H. Deka, I. Ritacco, N. Fridman, L. Caporaso and M. S. Eisen, Catalytic Regeneration of Metal-Hydrides from Their Corresponding Metal-Alkoxides via the Hydroboration of Carbonates to Obtain Methanol and Diols, *Chem. Sci.*, 2023, **14**, 8369–8379.
30 K. Makarov, A. Kaushansky and M. S. Eisen, Catalytic Hydroboration of Esters by Versatile Thorium and Uranium Amide Complexes, *ACS Catal.*, 2022, **12**, 273–284.
31 K. Makarov, I. Ritacco, N. Fridman, L. Caporaso and M. S. Eisen, Against All Odds, Uranium and Thorium Iminato Complexes Enable the Cleavage of C=O Bonds in Isocyanates, *ACS Catal.*, 2023, **13**, 11798–11814.
32 R. Kumar, N. J. Flodén, W. G. Whitehurst and M. J. Gaunt, A General Carbonyl Alkylative Amination for Tertiary Amine Synthesis, *Nature*, 2020, **581**, 415–420.
33 D. C. Blakemore, L. Castro, I. Churcher, D. C. Rees, A. W. Thomas, D. M. Wilson and A. Wood, Organic Synthesis Provides Opportunities to Transform Drug Discovery, *Nat. Chem.*, 2018, **10**, 383–394.
34 C. W. Cheung and X. Hu, Amine Synthesis via Iron-Catalysed Reductive Coupling of Nitroarenes with Alkyl Halides, *Nat. Commun.*, 2016, **7**, 12494.
35 J. M. Hooker, A. T. Reibel, S. M. Hill, M. J. Schueller and J. S. Fowler, One-Pot, Direct Incorporation of $[^{11}C]CO_2$ into Carbamates, *Angew. Chem., Int. Ed.*, 2009, **48**, 3482–3485.
36 R. Feng, Y.-Q. Zhen, D. Wu, L. Sun, J.-B. Xu, X. Li, L. Zhang and F. Gao, Late-Stage Modification of Complex Drug: Base-Controlled Pd-Catalyzed Regioselective Synthesis and Bioactivity of Arylated Osimertinibs, *Sci. Adv.*, 2024, **10**, 1–13.

37 A. K. Ghosh and M. Brindisi, Organic Carbamates in Drug Design and Medicinal Chemistry, *J. Med. Chem.*, 2015, **58**, 2895–2940.

38 R. F. Nystrom and W. G. Brown, Reduction of Organic Compounds by Lithium Aluminum Hydride. III. Halides, Quinones, Miscellaneous Nitrogen Compounds, *J. Am. Chem. Soc.*, 1948, **70**, 3738–3740.

39 H. Elsen, C. Färber, G. Ballmann and S. Harder, LiAlH 4 : From Stoichiometric Reduction to Imine Hydrogenation Catalysis, *Angew. Chem.*, 2018, **130**, 7274–7278.

40 Y. Zhang, F. Bohle, R. Bleith, G. Schnakenburg, S. Grimme and A. Gansäuer, Synthesis of 1,3—Amino Alcohols by Hydroxy–Directed Aziridination and Aziridine Hydrosilylation, *Angew. Chem.*, 2018, **130**, 13716–13720.

41 (*a*) S. J. Simpson, H. W. Turner and R. A. Andersen, Preparation and hydrogen-deuterium exchange of alkyl and hydride bis(trimethylsilyl)amido derivatives of the actinide elements, *Inorg. Chem.*, 1981, **20**, 2991–2995; (*b*) H. W. Turner, R. A. Andersen, A. Zalkin and D. H. Templeton, Chloro-, Methyl-, and (Tetrahydroborato) tris((Hexamethyldisilyl)amido)thorium(IV) and Uranium (IV): Crystal Structure of (Tetrahydroborato)tris ((Hexamethyldisilyl)amido)thorium(IV), *Inorg. Chem.*, 1979, **18**, 1221–1224; (*c*) S. J. Simpson and R. A. Andersen, Actinide-carbon bonds: insertion reactions of carbon monoxide, tert-butyl isocyanide, and tert-butyl cyanide into $[(Me_3Si)_2N]_2MCH_2Si(Me)_2NSiMe_3$, *J. Am. Chem. Soc.*, 1981, **103**, 4063–4066; (*d*) S. J. Simpson, H. W. Turner and R. A. Andersen, Hydrogen-deuterium exchange: perdeuteriohydridotris(hexamethyldisilylamido)thorium(IV) and -uranium(IV), *J. Am. Chem. Soc.*, 1979, **101**, 7728–7729; (*e*) A. Dormond, A. El Bouadili, A. Aaliti and C. Moise, Insertion of Carbonyl Compounds into Actinide–Carbon σ Bonds: Reactivity of $[(Me_3Si)_2)_2N]_2SiMe_3$, *J. Organomet. Chem.*, 1985, **288**, C1–C5.

42 I. S. R. Karmel, N. Fridman, M. Tamm and M. S. Eisen, Mono(Imidazolin-2-Iminato) Actinide Complexes: Synthesis and Application in the Catalytic Dimerization of Aldehydes, *J. Am. Chem. Soc.*, 2014, **136**, 17180–17192.

43 H. Liu, N. Fridman, M. Tamm and M. S. Eisen, Addition of E-H (E = N, P, C, O, S) Bonds to Heterocumulenes Catalyzed by Benzimidazolin-2-Iminato Actinide Complexes, *Organometallics*, 2017, **36**, 3896–3903.

44 A. Das and P. Mahanwar, A Brief Discussion on Advances in Polyurethane Applications, *Adv. Ind. Eng. Polym. Res.*, 2020, **3**, 93–101.

45 A. Kemona and M. Piotrowska, Polyurethane Recycling and Disposal: Methods and Prospects, *Polymers*, 2020, **12**, 1752.

46 G. Brereton, R. M. Emanuel, R. Lomax, K. Pennington, T. Ryan, H. Tebbe, M. Timm, P. Ware, K. Winkler, T. Yuan, Z. Zhu, N. Adam, G. Avar, H. Blankenheim, W. Friederichs, M. Giersig, E. Weigand, M. Halfmann, F.-W. Wittbecker, D.-R. Larimer, U. Maier, S. Meyer-Ahrens, K.-L. Noble and H.-G. Wussow, *Ullmann's Encyclopedia of Industrial Chemistry*, Wiley-VCH, 2019, pp. 1–76.

47 V. Zubar, A. T. Haedler, M. Schütte, A. S. K. Hashmi and T. Schaub, Hydrogenative Depolymerization of Polyurethanes Catalyzed by a Manganese Pincer Complex, *ChemSusChem*, 2022, **15**(1), e202101606.

48 G. Rossignolo, G. Malucelli and A. Lorenzetti, Recycling of Polyurethanes: Where We Are and Where We Are Going, *Green Chem.*, 2024, **26**, 1132–1152.

49 A. Sheel and D. Pant, Chemical Depolymerization of Polyurethane Foams via Glycolysis and Hydrolysis, in *Recycling of Polyurethane Foams*, Elsevier, 2018, pp. 67–75.

50 V. Goyal, N. Sarki, A. Narani, G. Naik, K. Natte and R. V. Jagadeesh, Recent Advances in the Catalytic N-Methylation and N-Trideuteromethylation Reactions Using Methanol and Deuterated Methanol, *Coord. Chem. Rev.*, 2023, **474**, 214827.